

Gravitational Lensing by NFW Halos

Candace Oaxaca Wright & Tereasa G. Brainerd
 Boston University, Department of Astronomy, Boston, MA 02215

ABSTRACT

We investigate the gravitational lensing properties of dark matter halos with Navarro, Frenk & White (NFW) density profiles and derive an analytic expression for the radial dependence of the shear, $\gamma(x)$, due to these objects. In addition, we derive an expression for the mean shear interior to a given radius, $\bar{\gamma}(x)$, and use this to quantify systematic errors that will arise in weak lensing mass estimates of astronomical objects in the case that the mass estimate is based on an *a priori* assumption that the underlying potential is that of a singular isothermal sphere when, in fact, the potential is that of an NFW-type object. On mass scales between $10^{11} M_{\odot} \lesssim M_{200} \lesssim 10^{15} M_{\odot}$, the assumption of an isothermal sphere potential results in an overestimate of the halo mass, and the amount by which the mass is overestimated increases linearly with the value of the NFW concentration parameter. Considerable overestimates of the mass ($\sim 60\%$) can occur for galaxy-sized halos, but for rich clusters the mass overestimate is small. The degree to which the mass is systematically in error is dependent upon the cosmology adopted, with a COBE-normalized standard CDM model yielding the largest systematic errors for a given true value of the halo mass.

Subject headings: cosmology: theory — dark matter — gravitational lensing — galaxies: clusters: general

1. Introduction

Several recent numerical investigations (e.g., Navarro, Frenk & White 1997, 1996, 1995) have indicated the existence of a universal density profile for dark matter halos that results from the generic dissipationless collapse of density fluctuations. Interior to the virial radius, the Navarro, Frenk & White (NFW) profile appears to be a very good description

of the radial mass distribution of simulated objects that span 9 orders of magnitude in mass (mass scales ranging from that of globular clusters to that of large galaxy clusters). The apparent generality of the NFW density profile has been confirmed independently by a number of studies (e.g., Bartelmann et al. 1998; Thomas et al. 1998, Carlberg et al. 1997; Cole & Lacey 1997; Kravtsov, Klypin & Khokhlov 1997; Tormen, Bouchet & White 1997); however, there are a few controversial claims that the NFW prescription may fail at very small radii (e.g., Ghigna et al. 1998; Moore et al. 1998).

The NFW density profile is given by

$$\rho(r) = \frac{\delta_c \rho_c}{(r/r_s)(1+r/r_s)^2}, \quad (1)$$

where $\rho_c = \frac{3H^2(z)}{8\pi G}$ is the critical density for closure of the universe at the redshift, z , of the halo, $H(z)$ is Hubble’s parameter at that same redshift, and G is Newton’s constant. The scale radius $r_s = r_{200}/c$ is a characteristic radius of the cluster, c is a dimensionless number known as the concentration parameter, and

$$\delta_c = \frac{200}{3} \frac{c^3}{\ln(1+c) - c/(1+c)} \quad (2)$$

is a characteristic overdensity for the halo. The virial radius, r_{200} , is defined as the radius inside which the mass density of the halo is equal to $200\rho_c$ (see, e.g., Navarro, Frenk & White 1997). The mass of an NFW halo contained within a radius of r_{200} is therefore

$$M_{200} \equiv M(r_{200}) = \frac{800\pi}{3} \rho_c r_{200}^3 = \frac{800\pi}{3} \frac{\bar{\rho}(z)}{\Omega(z)} r_{200}^3 \quad (3)$$

where $\bar{\rho}(z)$ is the mean mass density of the universe at redshift z and $\Omega(z)$ is the density parameter at redshift z .

Although it has not been proven categorically, it is certainly widely–thought that the masses of large galaxies, groups of galaxies, galaxy clusters, and superclusters are dominated by some form of dissipationless dark matter. Therefore, it would not be unreasonable to expect that the spherically–averaged density profiles of these objects would be approximated fairly well by NFW profiles. Observationally, the total masses and mass–to–light ratios of these objects are not constrained especially well at present; however, this situation is changing rapidly, due in large part to the fact that high–quality imaging of gravitational lens systems is yielding direct constraints on the nature of the mass distribution within the dark matter halos.

Observations of gravitational lensing provide powerful constraints on both the total mass and the mass distribution within the lens itself, owing to the fact that one essentially

uses photons emitted by objects more distant than the lens to trace the underlying gravitational potential of the lens directly. In particular, large clusters of galaxies (which are both massive and centrally–condensed) are especially good gravitational lens candidates, and detections of the coherent pattern of weak lensing shear due to a number of clusters has led to interesting constraints on the masses of these objects (e.g., Tyson, Wenk & Valdes 1990; Bonnet et al. 1994; Dahle, Maddox & Lilje 1994; Fahlman et al. 1994; Mellier et al. 1994; Smail et al. 1994, 1995, 1997; Tyson & Fischer 1995; Smail & Dickinson 1995; Kneib et al. 1996; Seitz et al. 1996; Squires et al. 1996ab; Bower & Smail 1997; Fischer et al. 1997; Fischer & Tyson 1997; Luppino & Kaiser 1997; Clowe et al. 1998; Hoekstra et al. 1998). Although more controversial than the results for lensing clusters, detections of systematic weak lensing of distant field galaxies by foreground field galaxies have been reported and these have been used to place constraints on the physical sizes and total masses of the dark matter halos of the lens galaxies (e.g., Brainerd, Blandford & Smail 1996; Griffiths et al. 1996; Ebbels 1998; Hudson et al. 1998; Natarajan et al. 1998). Additionally, a detection of the coherent weak lensing shear due to a supercluster has been reported recently (Kaiser et al. 1998).

Because of the apparent direct applicability of the NFW density profile to the dominant mass component of all of these objects, and because of the potential of observations of gravitational lensing to provide strong, direct constraints on the amount and distribution of dark matter within them, we investigate the lensing characteristics of dark matter halos with generic NFW–type density profiles in this paper. In §2 we compute the convergence and the shear profiles of NFW halos. In §3 we compare the mean shear induced by NFW lenses to that of simpler singular isothermal sphere (SIS) lenses and consider the implications of our results for possible systematic errors in lens masses that are determined in observational investigations which invoke an *a priori* assumption of an isothermal lens potential. A discussion of the results is presented in §4.

2. Convergence and Shear of an NFW Object

We perform all of our calculations below using the thin lens approximation, in which an object’s lensing properties can be computed solely from a scaled, 2-dimensional Newtonian potential. The thin lens approximation is valid in the limit that the scale size of the lens is very much less than the path length traveled by the photons as they propagate from the source to the lens and from the lens to the observer. In this case the lensing properties of an object are completely described by two quantities, the convergence, κ , and the shear, $\vec{\gamma}$. The names of these quantities are indicative of their effects upon a lensed image; the

convergence describes the isotropic focusing of light rays while the shear describes the effect of tidal gravitational forces. Convergence acting alone leads to an isotropic magnification or demagnification while the shear induces distortions in the shapes of lensed images.

If we define z to be the optic axis, then for a lens with a 3-dimensional potential $\Phi(D_d\vec{\theta}, z)$ we can formulate a conveniently-scaled potential as projected on the sky:

$$\psi(\vec{\theta}) = \frac{D_{ds}}{D_d D_s} \frac{2}{c^2} \int \Phi(D_d\vec{\theta}, z) dz. \quad (4)$$

Here $\vec{\theta}$ is a radius vector on the sky and D_d , D_s , and D_{ds} are, respectively, the angular diameter distances between the observer and the lens, the observer and the source, and the lens and the source. Under the definition of $\psi(\vec{\theta})$ above, the convergence and the components of the shear tensor may be written as straightforward combinations of second-order derivatives of ψ with respect to image plane coordinates $\vec{\theta} = (\theta_1, \theta_2)$,

$$\kappa(\vec{\theta}) = \frac{1}{2} \left(\frac{\partial^2 \psi}{\partial \theta_1^2} + \frac{\partial^2 \psi}{\partial \theta_2^2} \right) \quad (5)$$

$$\gamma_1(\vec{\theta}) = \frac{1}{2} \left(\frac{\partial^2 \psi}{\partial \theta_1^2} - \frac{\partial^2 \psi}{\partial \theta_2^2} \right) \quad (6)$$

$$\gamma_2(\vec{\theta}) = \frac{\partial^2 \psi}{\partial \theta_1 \partial \theta_2} = \frac{\partial^2 \psi}{\partial \theta_2 \partial \theta_1}. \quad (7)$$

The magnitude of the shear is simply $\gamma = |\vec{\gamma}| = \sqrt{\gamma_1^2 + \gamma_2^2}$ (e.g., Schneider, Ehlers & Falco 1992). In the limit of weak gravitational lensing, the convergence and shear are formally small (i.e., $\kappa \ll 1$, $\gamma \ll 1$), the ellipticity induced in the image of an intrinsically circular source due to lensing is of order $\gamma/2$, and the position angle of the lensed image ellipse is of order the phase of $\vec{\gamma}$ (e.g., Schramm & Kayser 1995; Seitz & Schneider 1997).

The local value of the convergence may be expressed simply as the ratio of the local value of the surface mass density to the critical surface mass density:

$$\kappa(\vec{\theta}) = \frac{\Sigma(\vec{\theta})}{\Sigma_c}, \quad (8)$$

where

$$\Sigma_c \equiv \frac{c^2}{4\pi G} \frac{D_s}{D_d D_{ds}} \quad (9)$$

(e.g., Schneider, Ehlers & Falco 1992) and c in the equation above is the velocity of light. The radial dependence of the surface mass density of a spherically symmetric lens such as

an NFW lens is obtained simply by integrating the 3-dimensional density profile along the line of sight,

$$\Sigma(R) = 2 \int_0^\infty \rho(R, z) dz, \quad (10)$$

where $R = D_d \sqrt{\theta_1^2 + \theta_2^2}$ is the projected radius relative to the center of the lens.

For convenience we will adopt a dimensionless radial distance, $x = R/r_s$. Integrating equation (1) along the line of sight, the radial dependence of the surface mass density of an NFW lens can then be written as:

$$\Sigma_{\text{nfw}}(x) = \begin{cases} \frac{2r_s \delta_c \rho_c}{(x^2-1)} \left[1 - \frac{2}{\sqrt{1-x^2}} \operatorname{arctanh} \sqrt{\frac{1-x}{1+x}} \right] & (x < 1) \\ \frac{2r_s \delta_c \rho_c}{3} & (x = 1) \\ \frac{2r_s \delta_c \rho_c}{(x^2-1)} \left[1 - \frac{2}{\sqrt{x^2-1}} \arctan \sqrt{\frac{x-1}{1+x}} \right] & (x > 1) \end{cases} \quad (11)$$

(e.g., Bartelmann 1996). The radial dependence of the convergence due to an NFW lens is then simply $\kappa_{\text{nfw}}(x) = \Sigma_{\text{nfw}}(x)/\Sigma_c$.

Since the NFW density profile is spherically symmetric, the radial dependence of the shear can be written as

$$\gamma_{\text{nfw}}(x) = \frac{\bar{\Sigma}_{\text{nfw}}(x) - \Sigma_{\text{nfw}}(x)}{\Sigma_c} \quad (12)$$

(e.g., Miralda–Escudé 1991) where $\bar{\Sigma}_{\text{nfw}}(x)$ is the mean surface mass density interior to the dimensionless radius x . In terms of this radius, then, the mean surface mass density of an NFW halo is given by

$$\bar{\Sigma}_{\text{nfw}}(x) = \frac{2}{x^2} \int_0^x x' \Sigma_{\text{nfw}}(x') dx' = \begin{cases} \frac{4}{x^2} r_s \delta_c \rho_c \left[\frac{2}{\sqrt{1-x^2}} \operatorname{arctanh} \sqrt{\frac{1-x}{1+x}} + \ln \left(\frac{x}{2} \right) \right] & (x < 1) \\ 4r_s \delta_c \rho_c \left[1 + \ln \left(\frac{1}{2} \right) \right] & (x = 1) \\ \frac{4}{x^2} r_s \delta_c \rho_c \left[\frac{2}{\sqrt{x^2-1}} \arctan \sqrt{\frac{x-1}{1+x}} + \ln \left(\frac{x}{2} \right) \right] & (x > 1) \end{cases} \quad (13)$$

and the radial dependence of the shear is, therefore,

$$\gamma_{\text{nfw}}(x) = \begin{cases} \frac{r_s \delta_c \rho_c}{\Sigma_c} g_<(x) & (x < 1) \\ \frac{r_s \delta_c \rho_c}{\Sigma_c} \left[\frac{10}{3} + 4 \ln \left(\frac{1}{2} \right) \right] & (x = 1) \\ \frac{r_s \delta_c \rho_c}{\Sigma_c} g_>(x) & (x > 1) \end{cases} \quad (14)$$

where the functions $g_{<,>}(x)$ above depend upon only the dimensionless radius x and are explicitly independent of the cosmology:

$$g_{<}(x) = \frac{8 \operatorname{arctanh} \sqrt{\frac{1-x}{1+x}}}{x^2 \sqrt{1-x^2}} + \frac{4}{x^2} \ln \left(\frac{x}{2} \right) - \frac{2}{(x^2-1)} + \frac{4 \operatorname{arctanh} \sqrt{\frac{1-x}{1+x}}}{(x^2-1)(1-x^2)^{1/2}} \quad (15)$$

$$g_{>}(x) = \frac{8 \arctan \sqrt{\frac{x-1}{1+x}}}{x^2 \sqrt{x^2-1}} + \frac{4}{x^2} \ln \left(\frac{x}{2} \right) - \frac{2}{(x^2-1)} + \frac{4 \arctan \sqrt{\frac{x-1}{1+x}}}{(x^2-1)^{3/2}}. \quad (16)$$

Equation (14) above can also be obtained straightforwardly from equations (7) through (11) of Bartelmann (1996). The radial dependence of the shear due to an NFW lens is shown in Fig. 1.

The shear due to a given lens (e.g., a cluster of galaxies) is computed directly from the coherent distortion pattern that it induces in the images of distant source galaxies. In the realistic observational limit of weak shear and a finite number of lensed images, a measurement of the mean shear interior to a radius x centered on the center of mass of the lens (i.e., $\bar{\gamma}(x)$) is more easily determined than the differential radial dependence of the shear (i.e., $\gamma(x)$). In the case of the NFW profile, the mean shear interior to a (dimensionless) radius x can be computed directly from equation (14) above:

$$\bar{\gamma}_{\text{nfw}}(x) = \frac{2}{x^2} \int_0^x x' \gamma(x') dx' = \frac{r_s \delta_c \rho_c}{\Sigma_c} \left[\frac{2}{x^2} \left(\int_0^1 g_{<}(x') x' dx' + \int_1^x g_{>}(x') x' dx' \right) \right]. \quad (17)$$

A useful fiducial radius interior to which one might measure the mean shear is the virial radius, $R = r_{200}$, or equivalently, interior to $x = (r_{200}/r_s) = c$, where c is the concentration parameter. For all masses of astrophysical interest c is greater than 1 and, therefore, the mean shear interior to the virial radius becomes

$$\bar{\gamma}_{\text{nfw}}(r_{200}) = \frac{r_s \delta_c \rho_c}{\Sigma_c} \left[\frac{2}{c^2} \left(\int_0^1 g_{<}(x') x' dx' + \int_1^c g_{>}(x') x' dx' \right) \right] \quad (18)$$

which we rewrite as

$$\bar{\gamma}_{\text{nfw}}(r_{200}) = \frac{r_s \rho_c}{\Sigma_c} \mathcal{F}(c), \quad (19)$$

where

$$\mathcal{F}(c) = \delta_c \left[\frac{2}{c^2} \left(\int_0^1 g_{<}(x') x' dx' + \int_1^c g_{>}(x') x' dx' \right) \right] \quad (20)$$

is a function of the concentration parameter alone.

3. Comparison to the Singular Isothermal Sphere

Like the NFW mass profile, the singular isothermal sphere (SIS) mass profile is characterized by a single parameter (i.e., the velocity dispersion, σ_v). The mass of an SIS interior to a three dimensional radius r is:

$$M(r) = \frac{2\sigma_v^2 r}{G} \quad (21)$$

(e.g., Binney & Tremaine 1987) and the mean gravitational lensing shear interior to a radius R that is induced by an SIS lens is:

$$\bar{\gamma}_{\text{sis}}(R) = \frac{1}{\Sigma_c} \frac{\sigma_v^2}{GR} \quad (22)$$

(e.g. Schneider, Ehlers & Falco 1992).

Because of its simplicity, the SIS density profile is sometimes adopted in observational investigations in order to obtain an estimate of the mass of a lens without fully reconstructing its true underlying density profile (e.g., Tyson, Wenk & Valdes 1990; Bonnet et al. 1994; Smail et al. 1994, 1997; Smail & Dickinson 1995; Bower & Smail 1997; Fischer & Tyson 1997). By assuming that the underlying potential of the lens is well–approximated by an SIS, a measurement of the mean shear interior to a projected radius R leads directly to a measurement of the velocity dispersion of the lens (e.g., equation 22), which in turn leads directly to an estimate of the mass of the lens (e.g., equation 21).

The NFW density profile, which is shallower than isothermal on small scales, and which turns over to isothermal on large scales has, however, been shown to be a far better approximation than the SIS to the spherically–averaged density profiles of halos formed via dissipationless collapse. Therefore, it is likely that lens mass estimates based on an *a priori* assumption of an isothermal potential will be systematically in error. In this section we compare the mean shear induced by NFW lenses to that induced by SIS lenses, under the constraint that the NFW and SIS lenses both have identical virial radii, r_{200} , and, therefore, identical masses interior to r_{200} . From this we will then investigate the possible systematic errors in lens mass estimates that would arise due to the assumption of an isothermal potential when, in fact, the lens is best represented by an NFW density profile.

Let us consider two lenses which have identical masses, M_{200} , interior to the virial radius. One of the lenses has an NFW density profile with a concentration parameter of c and the other is a singular isothermal sphere with velocity dispersion σ_v . If these two objects have identical redshifts, z_d , and act as lenses for populations of source galaxies which have identical redshifts, z_s , then from equations (19) and (22) above, the ratio of the

mean shears induced by these two lenses interior to r_{200} is given by:

$$\frac{\bar{\gamma}_{\text{nfw}}(r_{200})}{\bar{\gamma}_{\text{sis}}(r_{200})} = \frac{r_s \rho_c r_{200}}{\sigma_v^2} G\mathcal{F}(c). \quad (23)$$

Using equations (3) and (21) above and recalling that the concentration parameter is $c = r_{200}/r_s$, it is straightforward to show that equation (23) reduces to

$$\frac{\bar{\gamma}_{\text{nfw}}(r_{200})}{\bar{\gamma}_{\text{sis}}(r_{200})} = \frac{3}{400\pi} \frac{\mathcal{F}(c)}{c}, \quad (24)$$

which is a function solely of the concentration parameter of the NFW lens and is explicitly independent of the redshift of the sources, z_s . Because of the dependence of the concentration parameter on both the redshift of the lens and the cosmology through $\bar{\rho}(z_d)$, equation (24) is not explicitly independent of either the cosmology or the lens redshift, z_d . However, for lenses of a given mass, its dependence on both z_d and the cosmology is relatively weak.

Shown in Figs. 2 and 3 are the ratio of the mean shears interior to r_{200} for NFW and SIS lenses with virial masses in the range of $10^{11}M_\odot \leq M_{200} \leq 10^{16}M_\odot$. Fig. 2 shows the results for lenses located at $z_d = 0.1$ and Fig. 3 shows the results for lenses located at $z_d = 0.5$. The four panels in the figures show the effects of varying the cosmology, and plotted along the top axes of all of the panels is the NFW concentration parameter which corresponds to the lens mass plotted on the lower axes.

Two of the cosmologies illustrated in Figs. 2 and 3 are standard cold dark matter (CDM) cosmologies, which differ from one another only in the choice of the normalization of the power spectrum (SCDM–I is a cluster abundance normalization while SCDM–II is COBE-normalized). The other two cosmologies are an open CDM model with zero cosmological constant (OCDM) and a spatially flat, low matter density CDM model with a large cosmological constant (Λ CDM). The parameters adopted for each of the models are summarized in Table 1 where $\Lambda_0 = \lambda/3H_0^2$, $H_0 = 100h$ km/s/Mpc, n is the index of the primordial power spectrum of density fluctuations and

$$\sigma_8 \equiv \left\langle \left[\frac{\delta\rho}{\rho}(8h^{-1}\text{Mpc}) \right]^2 \right\rangle^{\frac{1}{2}}. \quad (25)$$

Table 1: Cosmological Model Parameters

	Ω_0	Λ_0	h	σ_8	n
SCDM–I	1.0	0.0	0.50	0.63	1.0
SCDM–II	1.0	0.0	0.50	1.20	1.0
OCDM	0.25	0.0	0.70	0.85	1.0
Λ CDM	0.25	0.75	0.75	1.30	1.0

The FORTRAN program *charden.f*, written and generously provided by Julio Navarro, was used to calculate the values of the concentration parameters for the NFW lenses in the above cosmologies. For each of the cosmologies, c was determined for halos with masses in the range of $10^{11}M_\odot \leq M_{200} \leq 10^{16}M_\odot$ at redshifts of $z_d = 0.1$ and $z_d = 0.5$. These values of c were then used in conjunction with equation (24) to compute the ratio of the NFW to SIS mean shear interior to the virial radius.

For a given cosmology, it is clear by comparing Fig. 2 with Fig. 3 that equation (24) is only weakly dependent on the lens redshift, z_d . The largest difference between the various panels in Figs. 2 and 3 which correspond to identical cosmologies occurs for SCDM lenses with masses $\sim 10^{11}M_\odot$, and in this case the difference between $z_d = 0.1$ and $z_d = 0.5$ is only $\sim 10\%$. Similarly, by comparing the results plotted in all of the individual panels of Fig. 2 and Fig. 3 at fixed z_d , it is clear that equation (24) is not tremendously sensitive to the cosmology. In particular, the Λ CDM, OCM, and SCDM–I models all yield functions with nearly identical amplitudes for a given value of z_d . The SCDM–II model yields a function which is somewhat higher than the other three models, exceeding the others by $\sim 25\%$ for halos with masses $\sim 10^{11}M_\odot$ and by $\sim 20\%$ for halos with masses $\sim 10^{16}M_\odot$.

Over the majority of the mass range investigated, the NFW lenses give rise to a mean shear interior to r_{200} which is systematically larger than that of the SIS lenses. As a result, if one were to measure the mean shear interior to a radius of r_{200} of an NFW halo, yet assume it to be an isothermal sphere, the resulting estimate of the virial mass of the lens (M_{200}) would be systematically high. From equations (21) and (22) above, it follows that the mass of an SIS lens interior to r_{200} is simply:

$$M_{200} = 2\Sigma_c r_{200}^2 \bar{\gamma}(r_{200}) \quad (26)$$

so that the mass inferred for the lens scales linearly with the mean shear. Therefore, the systematic error in the true virial mass of the lens is simply the ratio of the mean shear due to an NFW lens to that of an SIS lens with an identical amount of mass contained inside r_{200} (i.e., Figs. 2 and 3).

Shown in Fig. 4 is the ratio of the mean shear (interior to r_{200}) of an NFW lens and an SIS lens, plotted as a function of the NFW concentration parameter. (As in Figs. 2 and

3, both lenses have identical masses interior to r_{200}). From this figure, then, if one were to measure a mean shear for a given NFW lens, yet model the lens as an isothermal sphere, the degree of systematic error in an estimate of the virial mass would clearly be a function of the concentration parameter of the lens. For a given halo mass, the concentration parameter is a function of the cosmology (e.g., the top axes of Figs. 2 and 3); however, it is always the case that for a given cosmology, the larger the value of c , the lower is the value of M_{200} . The general conclusions that can be drawn from Fig. 4 are: [1] the lower the mass of an NFW halo, the larger the systematic error in the mass estimate if the lens is assumed to be an isothermal sphere and [2] for a halo of a given mass, the largest systematic error in the mass estimate occurs in a COBE-normalized cosmology (i.e., SCDM-II). With the exception of SCDM-II for which the error is somewhat larger, the systematic error in an estimate of M_{200} for rich clusters ($M_{200} \sim 10^{15} M_{\odot}$) is negligible ($\lesssim 10\%$). The systematic error in an estimate of M_{200} for galaxy-mass objects ($M_{200} \sim 10^{11} M_{\odot}$) is, on the other hand, considerable (of order 55% to 65% for the SCDM-II model and of order 30% to 40% for the other models).

4. Discussion

It is generally thought that the masses of large galaxies, galaxy groups, galaxy clusters, and superclusters are dominated by some form of dissipationless dark matter and, thus, it is not unreasonable to expect that their underlying mass density profiles will be represented reasonably well by NFW profiles. In addition, since their total masses and mass-to-light ratios are not strongly constrained at present, a significant effort is currently being devoted to the use of observations of gravitational lensing by these objects to quantify the amount and distribution of dark matter within them. We have, therefore, investigated the properties of NFW lenses in this paper and we have presented analytic expressions for the radial dependence of the convergence, $\kappa(x)$, and shear, $\gamma(x)$, due to dark matter halos which have NFW density profiles. We have also presented an expression for the mean shear interior to a given radius, $\bar{\gamma}(x)$, due to NFW lenses and we have compared the mean shear interior to the virial radius of an NFW lens to that yielded by a singular isothermal sphere lens with an identical virial mass.

It is not uncommon for the mass of a gravitational lens to be estimated under an assumption that the lens may be approximated by a singular isothermal sphere. However, it has been clearly demonstrated that the NFW density profile is a far better approximation to the density profile of objects formed by generic dissipationless collapse than is the isothermal sphere. We have computed the systematic error that would be encountered

in an estimate of the mass of an NFW lens, where the lens is assumed *a priori* to be an isothermal sphere. Over mass scales of $10^{11}M_{\odot} \lesssim M_{200} \lesssim 10^{15}M_{\odot}$, the mass of the NFW lens is systematically overestimated when it is assumed that, for a given measured value of $\bar{\gamma}(r_{200})$, the lens can be approximated by an isothermal sphere.

The size of the systematic error in the lens mass due to the isothermal sphere assumption is a function of the NFW concentration parameter of the lens, with the largest error occurring for halos with the largest values of c and, hence, with the smallest masses. The systematic error in the mass is not dramatic (i.e., not even as much as a factor of ~ 2), but this is unsurprising since the shape of the NFW density profile in the outer regions of the halo is fairly close to an isothermal profile.

In the case of halos with masses comparable to that of rich clusters, $M_{200} \sim 10^{15}M_{\odot}$, the systematic error in the mass due to the assumption of an isothermal potential is small. Therefore, the masses of lensing clusters that are estimated under the assumption of an isothermal potential (and in the limit that the shear is detected out to a radius that is large enough to be comparable to r_{200}) should not have large systematic errors if, indeed, their density profiles are fitted well by NFW profiles.

However, recent observations of lensing of distant field galaxies by nearby field galaxies (and, additionally, by the individual galaxies within clusters, e.g., Natarajan et al. 1998) have inspired a number of investigations through which the mass and extent of the dark matter halos of the lens galaxies might be constrained. The technique, known as galaxy–galaxy lensing, seems very promising at the moment, and in the near future a considerable amount of effort will be devoted to the use of observations of galaxy–galaxy lensing to constrain the nature of the dark matter halos of galaxies. The results of our investigation of systematic errors in the mass estimated for NFW lenses under the assumption of an isothermal potential indicate that these errors can be significant for galaxy–mass lenses ($\sim 60\%$ in the case of a COBE-normalized CDM universe). Therefore, in the upcoming studies of galaxy–galaxy lensing, should an observational constraint on the masses of galaxy halos be based upon the assumption of an isothermal potential, it will be important to keep such systematic errors in mind when judging the strength of such a constraint.

Acknowledgments

Support under NSF contract AST-9616968 (TGB and COW) and an NSF Graduate Fellowship (COW) are gratefully acknowledged.

REFERENCES

- Bartelmann, M. 1996, *A&A*, 313, 697
- Bartelmann, M., Huss, A., Colberg, J.M., Jenkins, A., & Pearce, F.R. 1998, *A&A*, 330, 1
- Binney, J. & Tremaine, S. 1987, *Galactic Dynamics* (Princeton: Princeton University Press)
- Bonnet, H., Mellier, Y. & Fort, B. 1994, *ApJ*, 427, L83
- Bower, R. G. & Smail, I. 1997, *MNRAS*, 290, 292
- Brainerd, T. G., Blandford, R. D. & Smail, I. 1996, *ApJ*, 466, 623
- Carlberg, R.G., Yee, H.K.C., Ellingson, E., Morris, S.L., Abraham, R., Gravel, P., Pritchet, C.J., Smecker-Hane, T., Hartwick, F.D.A., Hesser, J.E., Hutchings, J.B., & Oke, J.B. 1997, *ApJ*, 485, L13
- Clowe, D., Luppino, G. A., Kaiser, N., Henry, J. P. & Gioia, I. 1998, *ApJ*, 497, L61
- Cole, S. & Lacey, C. 1997, *MNRAS*, 281, 716
- Dahle, H., Maddox, S. J. & Lilje, P. B. 1994, *ApJ*, 435, L79
- Ebbels, T. 1998, PhD Thesis (Cambridge University)
- Fahlman, G., Kaiser, N., Squires, G. & Woods, D. 1994, *ApJ*, 289, L1
- Fischer, P., Bernstein, G., Rhee, G., & Tyson, J. A. 1997, *ApJ*, 113, 521
- Fischer, P. & Tyson, J. A. 1997, *AJ*, 114, 14
- Ghigna, S., Moore, B., Governato, F., Lake, G., Quinn, T., & Stadel, J. 1998, *MNRAS*, 300, 146
- Griffiths, R. E., Casertano, S., Im, M., & Ratnatunga, K. U. 1996, *MNRAS*, 282, 1159
- Hoekstra, H., Franx, M., Kuijken, K., & Squires, G. 1998, *ApJ*, 504, 636
- Hudson, M. J., Gwyn, S. D. J., Dahle, H., & Kaiser, N. 1998, *ApJ*, 503, 531
- Kaiser, N., Wilson, G., Luppino, G., Kofman, L., Gioia, I., Metzger, M., & Dahle, H. 1998, [astro-ph/9809268](#)
- Kneib, J.-P., Ellis, R. S., Smail, I., Couch, W. J., & Sharples, R. M. 1996, *ApJ*, 471, 643
- Kravtsov, A.V., Klypin, A.A., & Khokhlov, A.M. 1997, *ApJS*, 111, 73
- Luppino, G. & Kaiser, N. 1997, *ApJ*, 475, 20
- Mellier, Y., Dantel-Fort, M., Fort, B., & Bonnet, H. 1994, *A&A*, 289, L15
- Miralda-Escudé, J. 1991, *ApJ*, 370, 1
- Moore, B., Governato, F., Quinn, T. & Stadel, J. 1998, *ApJ*, 499, L5

- Natarajan, P., Kneib, J.-P., Smail, I., & Ellis, R. S. 1998, *ApJ*, 499, 600
- Navarro, J.F., Frenk, C.S. & White, S.D.M. 1995, *MNRAS*, 275, 720
- Navarro, J.F., Frenk, C.S. & White, S.D.M. 1996, *ApJ*, 462, 563
- Navarro, J.F., Frenk, C.S. & White, S.D.M. 1997, *ApJ*, 490, 493
- Schneider, P., Ehlers, J. & Falco, E.E. 1992, *Gravitational Lenses*. Berlin: Springer-Verlag
- Schramm, D. & Kayser, R. 1995, *A&A*, 299,1
- Seitz, C., Kneib, J.-P., Schneider, P., & Seitz, S. 1996, *A&A*, 314, 707
- Seitz, C. & Schneider, P. 1997, *A&A*, 318, 687
- Smail, I. & Dickinson, M. 1995, *ApJ*, 455, L99
- Smail, I., Ellis, R. S., Fitchett, M. J. 1994, *MNRAS*, 270, 245
- Smail, I., Ellis, R. S., Fitchett, M. J., & Edge, A. C. 1995, *MNRAS*, 273, 277
- Smail, I., Ellis, R. S., Dressler, A., Couch, W., Oemler, A., Sharples, R. M., & Butcher, H. 1997, *ApJ*, 479, 70
- Squires, G., Kaiser, N., Babul, A., Fahlman, G., Woods, D., Neumann, D. M., & Böhringer, H. 1996a, *ApJ*, 461, 572
- Squires, G., Kaiser, N., Fahlman, G., Babul, A., & Woods, D. 1996b, *ApJ*, 469, 73
- Thomas, P.A., Colberg, J.M., Couchman, H.M.P., Efstathiou, G.P., Frenk, C.S., Jenkins, A.R., Nelson, A.H., Hutchings, R.M., Peacock, J.A., Pearce, F.R., & White, S.D.M. 1998, *MNRAS*, 296, 1061
- Tormen, G., Bouchet, F.R., & White, S.D.M. 1997, *MNRAS*, 286,865
- Tyson, A. & Fischer, P. 1995, *ApJ*, 446, L55
- Tyson, J. A., Wenk, R. A. & Valdes, F. 1990, *ApJ*, 349, L1

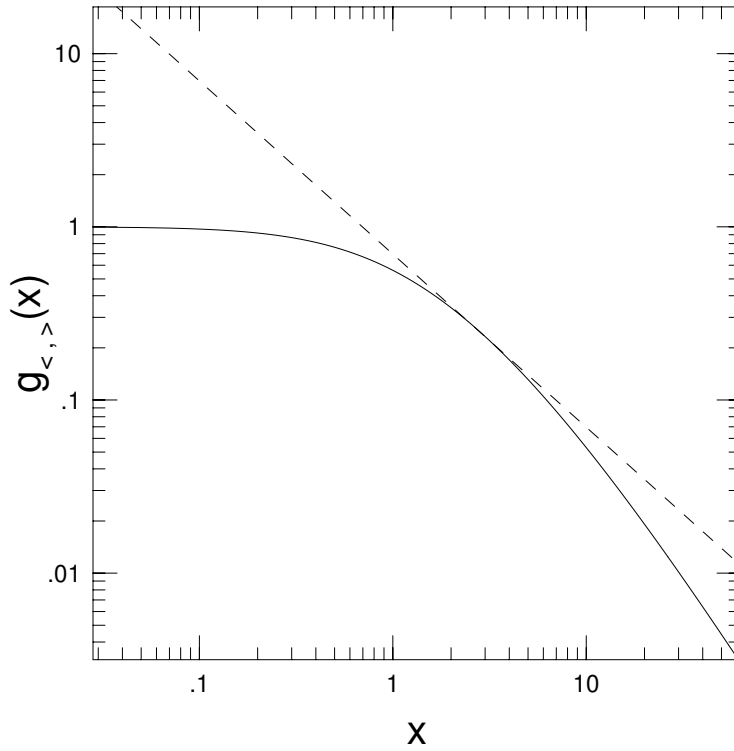


Fig. 1.— Solid line: the dependence of γ_{nfw} on the dimensionless radius $x = R/r_s$, i.e., equations (15) and (16). Also shown for comparison (dashed line) is the radial dependence of the shear due to a singular isothermal lens, $\gamma_{\text{sis}}(x) \propto x^{-1}$. The normalization is arbitrary.

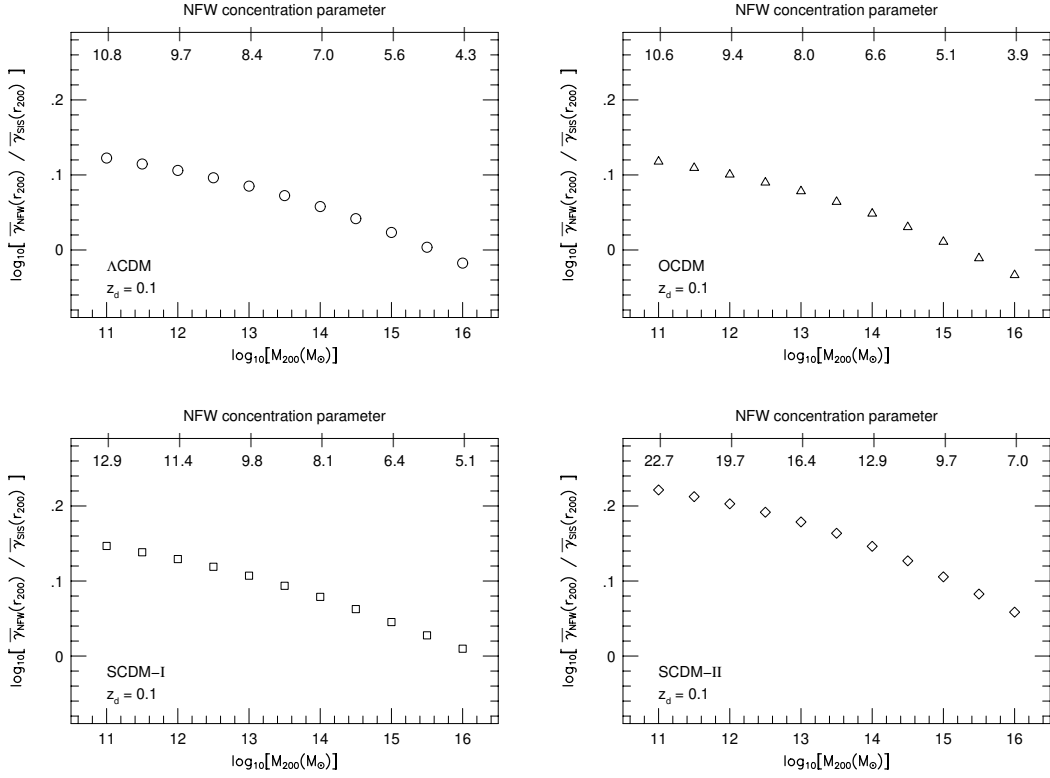


Fig. 2.— Ratio of the mean shear interior to a radius of r_{200} for NFW and SIS lenses. Both lenses are constrained to have identical masses interior to r_{200} (see text). The panels correspond to four different CDM models, and in this figure all of the lenses were placed at redshift of $z_d = 0.1$.

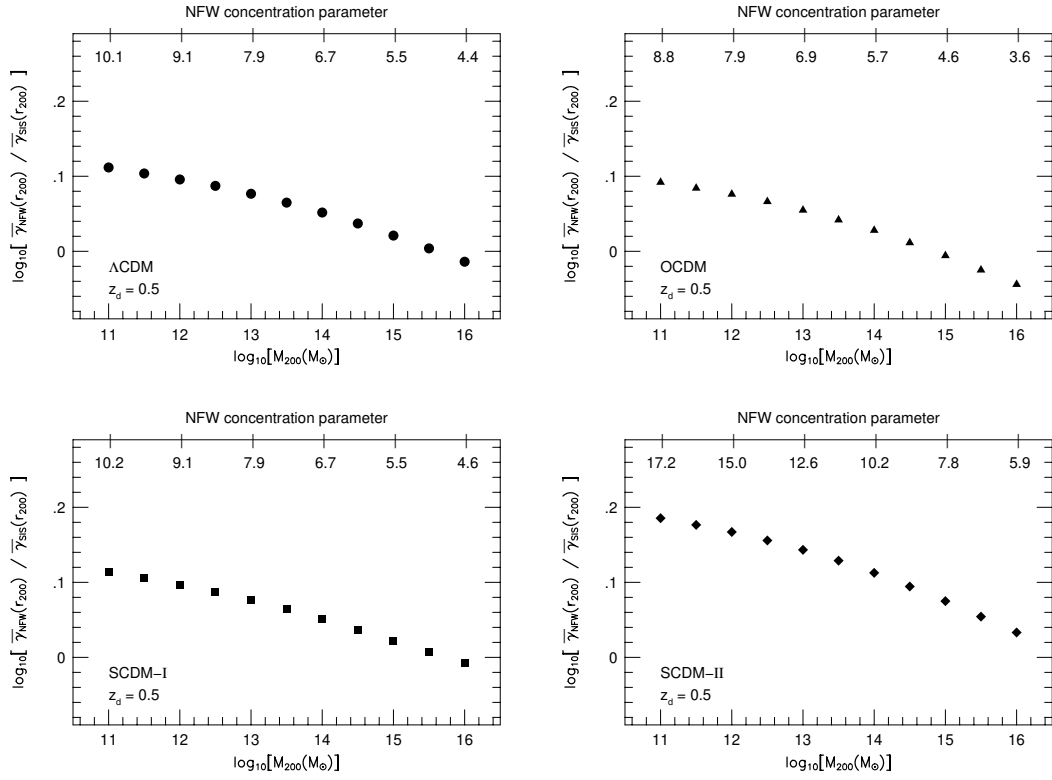


Fig. 3.— Same as Fig. 2, but the lenses were placed at a redshift of $z_d = 0.5$

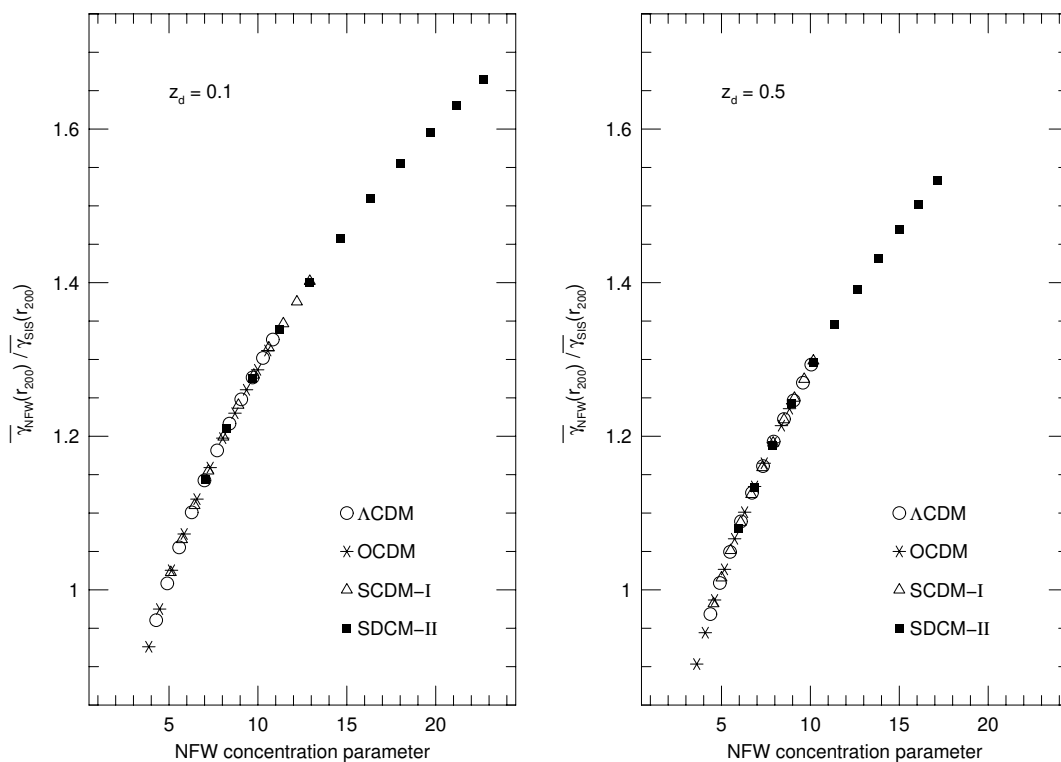


Fig. 4.— Ratio of the mean shear interior to a radius of r_{200} for NFW and SIS lenses as a function of the halo concentration parameter. The point types refer to four different CDM models. The left panel shows the result obtained when all lenses are placed at a redshift of $z_d = 0.1$; the right panel shows the result obtained when all lenses are placed at a redshift of $z_d = 0.5$.